# Drift mobility of long-living excitons in coupled GaAs quantum wells

A. Gärtner,[1] A. W. Holleitner,[1,*] D. Schuh,[2] and J. P. Kotthaus[1]

[1] *Department für Physik and Center for NanoScience, Ludwig-Maximilians-Universität, Geschwister-Scholl-Platz 1, D-80539 München, Germany*

[2] *Institut für Angewandte und Experimentelle Physik, Universität Regensburg, Universitätsstraße 31, D-93040 Regensburg, Germany* [†]

We observe high-mobility transport of indirect excitons in coupled GaAs quantum wells. A voltage-tunable in-plane potential gradient is defined for excitons by exploiting the quantum confined Stark effect in combination with a lithographically designed resistive top gate. Excitonic photoluminescence resolved in space, energy, and time provides insight into the in-plane drift dynamics. Across several hundreds of microns an excitonic mobility of $> 10^5\,\mathrm{cm}^2/\mathrm{eVs}$ is observed for temperatures below 10 K. With increasing temperature the excitonic mobility decreases due to exciton-phonon scattering.

The pioneering work of Keldysh and Kozlov in 1968 has triggered many experiments aiming to observe the bosonic nature of excitons in solid state systems.[1] For detecting the Bose-Einstein condensation of excitons, it is a prerequisite to define controllable confinement potentials for excitons. So far trapping of excitons has been demonstrated in strained systems,[2,3,4] magnetic traps,[5] "natural traps" defined by interface roughness fluctuations,[6] and electrostatic traps.[7,8,9,10] Only the latter enable in-situ control of the trapping potential. In addition, electrostatic traps can be extended towards optoelectronic solid-state devices due to their potential scalability and compatibility with existing semiconductor technology.

Here we investigate the drift dynamics of long-living excitons in coupled quantum wells (QWs) in a voltage-tunable semiconductor device. In prior experiments on coupled GaAs/AlAs-QWs a static, spatially resolved photoluminescence spectroscopy has been used to detect excitonic drift.[11] We extend this approach towards time-of-flight (TOF) experiments in coupled GaAs-QWs by detecting the excitonic photoluminescence (PL) as a function of space, energy, and time. The technique relies on the quantum confined Stark effect (QCSE), and it allows distinguishing the dynamics of excitons from electron-hole effects.[9] In a field effect structure such as shown in Fig. 1(a), electrons and holes of photogenerated excitons may rearrange in a way that they are spatially separated by the tunnel barrier between the GaAs-QWs. These indirect excitons have a lifetime of $\sim 300\,\mathrm{ns}$ (for perpendicular electric fields of $\sim 10^6\,\mathrm{V/m}$),[12] while the lifetimes of direct excitons are in the order of 1 ns.[13] The excitonic drift of such indirect, long-living excitons is induced by applying a voltage $U_\Delta$ across a resistive top gate (Fig. 1(a)). Hereby, the electric field perpendicular to the QWs is laterally varied, and due to the QCSE, mobile excitons drift along the gradient towards regions of high electric field (Fig. 1(b)).[7,11] In the TOF-experiments we find excitonic mobilities $\geq 10^5\,\mathrm{cm}^2/\mathrm{eVs}$ and scattering times $\geq 10$ ps at low temperatures. Both values exceed previous results on coupled QWs by a factor of 200.[11] For temperatures higher than 10 K the excitonic drift is limited by phonon-scattering processes.

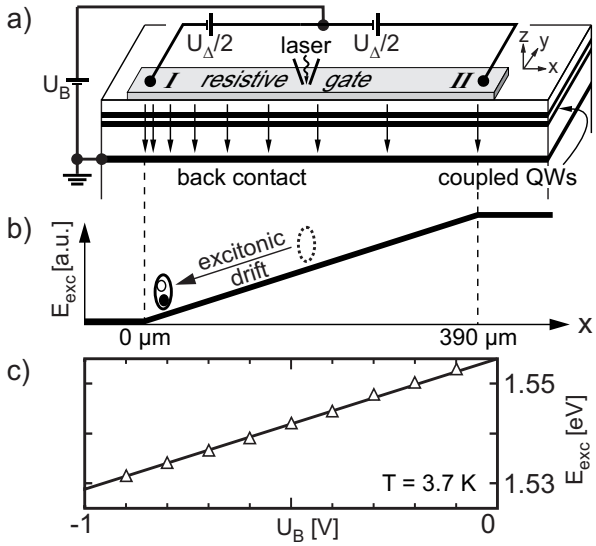


FIG. 1: (a) Excitonic time-of-flight apparatus. A current-carrying top gate (grey) defines a laterally varying vertical electric field (vertical arrows). (b) Sketch of the in-plane excitonic potential between contacts "I" and "II" due to the quantum confined Stark effect (QCSE). The slope of the gradient is tunable via the voltage $U_\Delta$. (c) Calibration of the QCSE-shift by application of a dc-voltage $U_\mathrm{B}$ to the top gate.

Starting point is an epitaxially grown AlGaAs/GaAs-heterostructure containing two GaAs-QWs encompassed by AlGaAs barriers (Fig. 1(a)). Each QW has a thickness of 8 nm, while the QWs are separated by a 4 nm-thick tunnel barrier made out of $Al_{0.3}Ga_{0.7}As$. The QWs are located 60 nm below the surface of the heterostructure. An n-doped GaAs-layer at a depth of $d = 370\,\mathrm{nm}$ serves as back gate, and a semi-transparent titanium layer is used as the top gate of the field effect structure. The metal gates, prepared by standard optical lithography, have typically a thickness of 10 nm, a width of 50 $\mu$m, and a length ranging between 500 $\mu$m and 1000 $\mu$m. The resistance of such a gate strip is between 2 k$\Omega$ and 4 k$\Omega$ depending on its length.

The excitonic drift experiments are carried out in a helium continuous-flow cryostat in combination with a

micro-photoluminescence setup in the temperature range between 3.5 K and 40 K. The excitons are locally excited by focusing a pulsed laser onto the center of the top gate. The laser is operated at a pulse length of 50 ns and at a repetition period of 10 $\mu$s. At a spot diameter of $\approx 10\,\mu$m the power density is 5 kW/cm$^2$. The laser wavelength is chosen to be 680 nm, such that electron-hole-pairs are only created in the GaAs-QWs and not in the AlGaAs-barriers. For the TOF experiments, the PL signal of the recombining excitons is picked up by the optical microscope as a function of the time-delay with respect to the initial laser pulse. The optical signal is subsequently guided through a triple-grating imaging spectrometer. An attached fast-gated, intensified CCD (charge coupled device) camera with an exposure time of 5 ns detects the PL emission of the excitonic cloud as a function of energy and space. In order to yield a sufficient signal to noise ratio, all images shown are taken by integrating over $2 \times 10^7$ single events.

In Fig. 1(c) we calibrate the shift of the exciton energy due to the QCSE as a function of the applied voltage $U_\mathrm{B}$ at $U_\Delta = 0$ V. The energy $\mathrm{E_{exc}}$ of the spatially indirect excitons is shifted to lower values by $\delta\mathrm{E_{exc}} = ed \times E_z$, with $d$ the center distance of the two QWs and $E_z$ the electric field perpendicular to the QWs. The data in Fig. 1(c) nicely follow a linear dependence with a slope of $\partial\mathrm{E_{exc}}/\partial U = 26.4$ meV/V. The red-shift is independent of the bath temperature $T$ up to 30 K. For the TOF experiments, a constant bias voltage $U_\mathrm{B}$ of $-0.4$ V is applied to the top gate with respect to the grounded back contact at all times. 50 ns after the laser has been switched off, all short-living direct excitons have decayed and only indirect excitons remain. Due to diffusion such a cloud of mobile indirect excitons has typically a FWHM-diameter of about 80 $\mu$m, in accordance with previous results.[14,15]

We define $t = 0$ as the point of time when the voltage drop $U_\Delta$ is applied across the resistive gate strip. In turn, the voltage between contacts "I" and "II" increases linearly along the gate strip. This voltage configuration creates a QCSE-mediated excitonic gradient potential $\mathrm{E_{exc}}$ as sketched in Fig. 1(b). In turn, the excitons are exposed to a force $F = -\nabla\mathrm{E_{exc}} = ed\nabla|E_z|$.[12] Since $U_\Delta$ is widely tunable, the method allows studying the in-plane drift of indirect excitons at different velocities. Fig. 2 shows three subsequent CCD-snapshots with 5 ns exposure time for $U_\Delta = 2$ V at (a) $t = 0$, (b) $t = 20$ ns, and (c) $t = 40$ ns. Each image exhibits the lateral distribution of the excitons resolved in space (vertical axis) and in energy (horizontal axis). The distributions are tilted off the horizontal orientation in all snapshots, proving that the gate strip creates an in-plane gradient of the excitonic energy. Under the given experimental conditions, the linear gradient $\nabla\mathrm{E_{exc}} \approx 100\,\mu$eV/$\mu$m obtained from the tilt in Fig. 2(b) and (c) agrees well with the value for the dc-QCSE energy shift presented in Fig. 1(c). The lower energy gradient in Fig. 2(a) is due to an $RC$-constant of the resistive gate of $< 10$ ns which governs the raising behaviour of $U_\Delta$.

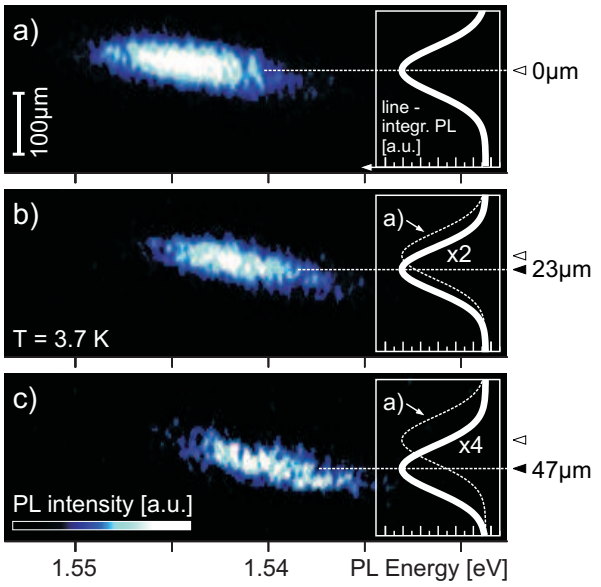


FIG. 2: Photoluminescence images showing drift of excitons at $T = 3.7$ K; taken at $t = 0$ ns (a), $t = 20$ ns (b), and $t = 40$ ns (c) after enabling the excitonic gradient potential. Insets: Energy-integrated representations of the data (solid curves). In the insets of (b) and (c) the lateral PL distribution of the cloud at $t = 0$ ns is shown as a dashed curve.

In Fig. 2(b)[(c)] the center of the excitonic cloud has travelled $(23.3 \pm 1.1)\,\mu$m [$(47.4 \pm 1.8)\,\mu$m] away from the excitation spot towards electrode "I" as defined in Fig. 1(a). At the same time, the excitons have reduced their energy by $\sim 2$ meV [$\sim 4$ meV]. As a function of the delay-time, the center of the excitonic distribution follows a diagonal path with respect to space and energy within the error bars (data not shown). The corresponding gradient $\partial\mathrm{E_{exc}}/\partial U \approx 25$ meV/V again agrees well with the gradient obtained from the dc-measurements in Fig. 1(c). This experimental finding proves that we study the drift dynamics specifically of indirect excitons. In addition, we would like to note that due to the finite lifetime of the indirect excitons the PL intensity in Fig. 2(b) and 2(c) has decreased by a factor of 2 and 4, respectively.

By following the temporal evolution of the center of the cloud in Fig. 2, the excitonic drift velocity $v_\mathrm{d}$ can be directly determined. Fig. 3(a) shows the dependence of $v_\mathrm{d}$ on the voltage drop $U_\Delta$ for various bath temperatures. At low temperatures we observe a maximum velocity of about $\sim 2.5 \times 10^3$ m/s. Experimentally, a leakage current $I_\mathrm{L}$ between the top and the back gate limits further increase of $U_\Delta$ and thus $v_\mathrm{d}$. For $U_\Delta \leq 2.5$ V we find $I_\mathrm{L}$ to be $\leq 1\,\mu$A. In this regime, a linear fit of the data gives the differential mobility $\mu_\mathrm{exc}$ of the excitons defined as

$$\mu_\mathrm{exc} = L \cdot (\mathrm{d}v_\mathrm{d}/\mathrm{d}U_\Delta) \cdot (-\partial\mathrm{E_{exc}}/\partial U)^{-1} \,. \qquad (1)$$

Fig. 3(b) summarizes the differential mobility $\mu_\mathrm{exc}$ of indirect excitons at various temperatures. At low temperature, a constant mobility $\mu_\mathrm{const}$ larger than $10^5$ cm$^2$/eVs is observed, which exceeds previous results by a fac-

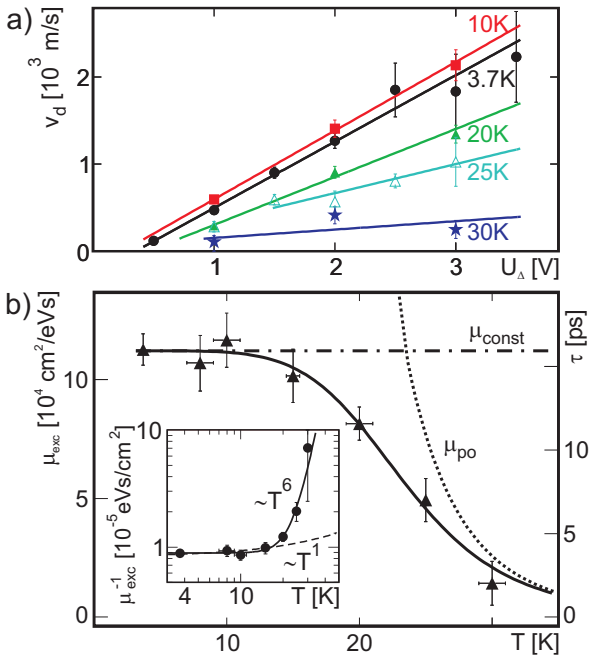


FIG. 3: (a) Measured excitonic drift velocity $v_\mathrm{d}$ versus the voltage drop $U_\Delta$ at various bath temperatures $T$. The differential mobility is obtained from linear curves fitted to the data. (b) Excitonic mobility $\mu_\mathrm{exc}$ and scattering time $\tau$ (right vertical axis) as a function of the temperature. Inset: double logarithmic representation of the inverse mobility $1/\mu_\mathrm{exc}$ versus temperature. Solid lines are theoretical fits to the data.

tor $\geq$ 200.[11] Recent publications on GaAs-QWs suggest that the maximum mobility in our experiment is only limited by barrier alloy scattering,[16] which is independent of temperature (dashed dotted line). With increasing temperature the excitonic mobility decreases as $\mu_\mathrm{po} \propto T^{-6}$ (dotted line), which is usually referred to enhanced scattering of excitons by polar optical phonons.[17] The combination of both scattering processes according to Matthiessen's rule explains the experimental data well (solid line). We would like to note that polar optical phonon scattering is usually expected for temperatures above 100 K.[17] However, as seen in the inset of Fig. 3(b), acoustic phonon scattering ($\propto T^{-1}$) cannot explain the data (dashed line).[16] Assuming an effective exciton mass $m^*_\mathrm{exc} = (m^*_\mathrm{e} + m^*_\mathrm{h}) \approx 0.25\, m_\mathrm{e}$ with $m^*_\mathrm{e,h}$ the effective electron/hole mass in GaAs and $m_\mathrm{e}$ the free electron mass, we can further estimate the transport scattering time to be $\tau \equiv \mu_\mathrm{exc} \cdot m^*_\mathrm{exc}$ (right axis in Fig. 3(b)). Since the PL signal depends on the temperature as well, TOF experiments above 30 K are ambiguous. Generally, the data shown are obtained from different samples patterned on one AlGaAs/GaAs-wafer. Since the electron mobility is proportional to the sixth power of the QW width,[18] future experiments will aim towards wider QWs.

In summary, we explore the quantum confined Stark effect in combination with a resistive top gate to study drift dynamics of indirect excitons in coupled GaAs quantum wells. The emitted photoluminescence of the drifting excitons is resolved in space, energy, and time, which allows measuring the drift velocity and mobility of the excitons. At low temperatures we observe a maximum mobility of $10^5\,\mathrm{cm}^2/\mathrm{eVs}$ which is a factor of 200 times larger than previous results on long-living excitons in coupled quantum wells.

We thank S. Manus and L. Prechtel for technical assistance and the Deutsche Forschungsgemeinschaft for financial support.

* Author to whom correspondence should be addressed; E-Mail: Alex.Holleitner@physik.uni-muenchen.de
† former address: Walter Schottky Institut, Technische Universität München, Am Coulombwall 3, D-85748 Garching, Germany

[1] L. V. Keldysh, A. N. Kozlov, Sov. Phys. JETP **27**, 521 (1968).
[2] D. P. Trauernicht, A. Mysyrowicz, J. P. Wolfe, Phys. Rev. B **28**, 3590 (1983).
[3] K. Kash, J. M. Worlock, M. D. Sturge. P. Grabbe, J. P. Harbison, A. Scherer, P. S. D. Lin, Appl. Phys. Lett. **53**, 782 (1988).
[4] V. Negotia, D. W. Snoke, K. Eberl, Appl. Phys. Lett. **75**, 2059 (1999).
[5] P. C. M. Christianen, F. Piazza, J. G. S. Lok, J. C. Maan, W. van der Vleuten, Physica B **249**, 624 (1998).
[6] L. V. Butov, C. W. Lai, A. L. Ivanov, A. C. Gossard, D. S. Chemla, Nature **417**, 47 (2002).
[7] S. Zimmermann, A. O. Govorov, W. Hansen, J. P. Kotthaus, M. Bichler, W. Wegscheider, Phys. Rev. B **56**, 13414 (1997).
[8] T. Huber, A. Zrenner, W. Wegscheider, M. Bichler, Phys. Stat. Sol. (a) **166**, R5 (1998).
[9] J. Krauß, A. Wixforth, A. V. Kalameitsev, A. O. Govorov, W. Wegscheider, J. P. Kotthaus, Phys. Rev. Lett. **88** (2002) 036803.
[10] A. T. Hammack, N. A. Gippius, G. O. Andreev, L. V. Butov, M. Hanson, A. C. Gossard, arXiv:cond-mat/0504045 (2005).
[11] M. Hagn, A. Zrenner, G. Böhm, G. Weimann, Appl. Phys. Lett. **67**, 232 (1995).
[12] A. Gärtner, D. Schuh, J. P. Kotthaus, Physica E (in press).
[13] J. Feldmann, G. Peter, E. O. Göbel, P. Dawson, K. Moore, C. Foxon, R. J. Elliott, Phys. Rev. Lett. **59**, 2337 (1987).
[14] Z. Vörös, R. Balili, D. W. Snoke, L. Pfeiffer, K. West, Phys. Rev. Lett. **94**, 226401 (2005).
[15] L. S. Levitov, B. D. Simons, L. V. Butov, Phys. Rev. Lett. **94**, 176404 (2005).
[16] H. Hillmer, A. Forchel, S. Hansmann, M. Morohashi, E. Lopez, H. P. Meier, K. Ploog, Phys. Rev. B **39**, 10901 (1989); and references therein.
[17] P.K. Basu, P. Ray, Phys. Rev. B **44**, 1844 (1991).
[18] H. Sasaki, T. Noda, K. Hirakawa, M. Tanaka, and T. Matsusue, Appl. Phys. Lett. **51**, 1934 (1987).